

# Not All Adapters Matter: Selective Adapter Freezing for Memory-Efficient Fine-Tuning of Language Models

Anonymous ACL submission

## Abstract

Transformer-based large-scale pre-trained models achieve great success, and fine-tuning, which tunes a pre-trained model on a task-specific dataset, is the standard practice to utilize these models for downstream tasks. Recent work has developed adapter-tuning, but these approaches either still require a relatively high resource usage. Through our investigation, we show that each adapter in adapter-tuning does not have the same impact on task performance and resource usage. Based on our findings, we propose SAFE, which gradually freezes less-important adapters that do not contribute to adaptation during the early training steps. In our experiments, SAFE reduces memory usage, computation amount, and training time by 42.85%, 34.59%, and 11.82%, respectively, while achieving comparable or better performance compared to the baseline. We also demonstrate that SAFE induces regularization effect, thereby smoothing the loss landscape.

## 1 Introduction

Large-scale pre-trained language models (PLMs) have manifested superior performance in various tasks (Kenton and Toutanova, 2019; Liu et al., 2019; Radford et al., 2019; Yang et al., 2019). However, training a PLMs from the scratch is usually time-consuming and resource-intensive. Common practice has been hence to fine-tune the large-scale pre-trained models by adapting all the parameters with the downstream tasks, i.e., full parameter fine-tuning (full-tuning).

Recently, Parameter-Efficient Fine-Tuning (PEFT), which focuses on optimizing a small fraction of parameters for downstream tasks, is receiving much attention (Houlsby et al., 2019; Lester et al., 2021; Li and Liang, 2021; Liu et al., 2022, 2023). Among various PEFT strategies, adapter-tuning has emerged as a prevalent method. It integrates lightweight modules, termed adapters,

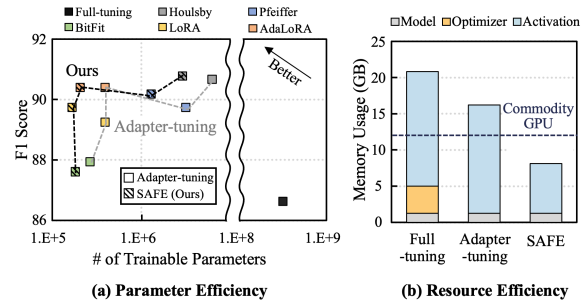


Figure 1: Comparison between full-parameter fine-tuning, adapter-tuning and our proposed SAFE on the BERT<sub>large</sub> model with SQuAD dataset. SAFE significantly reduces memory usage while providing comparable accuracy to adapter-tuning.

into each layer of PLMs and only tunes the adapters with the downstream tasks. As shown in Figure 1(a), the adapter-tuning methods (Houlsby et al., 2019; Pfeiffer et al., 2021; Zaken et al., 2022; Hu et al., 2021; Zhang et al., 2022), significantly reduce the number of trainable parameters, compared to the full-tuning, while exhibiting better performance for a downstream task.

As adapter-tuning reduces the number of trainable parameters, it is also expected to reduce the resource (i.e., memory) usage accordingly. Unfortunately, parameter-efficiency does not always translate into resource-efficiency. As shown in Figure 1(b), although adapter-tuning significantly reduces the number of trainable parameters (by 99.37%, on average) compared to the full-tuning, the memory usage is not much reduced (only by 22.19%, on average). This is because adapter-tuning does not reduce activation memory (i.e., intermediate values for reuse during backpropagation) which account for 76.00% of memory usage — it only reduces optimizer memory (e.g., gradients and momentum vectors). Considering the remarkable increase in model size compared to the modest increase in GPU memory capacity, adapter-tuning methods still face challenges in terms of

memory efficiency. For example, fine-tuning of a LLaMA-65B (Touvron et al., 2023) requires more than 780GB of GPU memory. As shown in Figure 1(b), enabling resource-efficient fine-tuning may enhance accessibility of fine-tuning to researchers and end-users, by reducing memory requirements below the capacity of commodity GPU memory.

According to previous work, the activation memory mostly depends on the backpropagation length (Chen et al., 2016; Rhu et al., 2016), which is determined by the number of adapters trained during the backward pass. Hence, to reduce the activation memory, it is crucial to reduce the number of training adapters. However, merely reducing the number of training adapters degrades accuracy. Here, a pivotal research problem arises:

### *Can we reduce the number of training adapters without sacrificing accuracy?*

To answer the question, we analyze the impact of individual adapters on the accuracy and resource usage of training (Figure 2 in Section 3). We observe that some adapters are being trained, even after they finish contributing to the accuracy improvement, occupying memory. Thus, it is possible to stop training (i.e., freezing) such adapters early if they do not contribute to the adaptation for a downstream task, de-allocating their activation memory. We also observe that such early freezing can even lead to the regularization effect on the model (Fu et al., 2023), improving the accuracy.

In this paper, we propose **SAFE** (Selective Adapter FrEeZing), which adaptively freezes adapters in the early epochs of training. In each epoch, SAFE identifies adapters that contribute relatively less to the accuracy improvement by using an importance score (Kornblith et al., 2019). It then freezes the adapters whose importance score is lower than a pre-defined threshold, reducing the memory usage and accelerating training time. By early freezing less important adapters, SAFE induces regularization effect on the model being trained, leading to a flatter loss surface. This is beneficial for finding an optimal point with higher generalization performance while optimizing neural network. In our evaluation, SAFE significantly reduces the average memory usage and TFLOPs by 46.89% and 51.73%, respectively, across various models and downstream tasks without compromising accuracy compared to the baseline, LoRA (Hu et al., 2021). SAFE even improves the accuracy for some tasks, compared to LoRA, by up to 4.33%

while reducing memory usage by 53.60%, by inducing the regularization effect.

In summary, our key contributions include:

- We uncover that adapters exhibit varying degrees of contribution to model adaptation and resource usage (Section 3).
- Motivated by this observation, we propose SAFE, a novel approach that enables resource-efficient fine-tuning by selectively early-freezing less important adapters (Section 4).
- Our evaluation on various downstream tasks demonstrates that SAFE not only achieves comparable or even better task performance to baselines but also significantly reduces resource usage by inducing the regularization effect on the model (Section 5).

## 2 Related Work

**Parameter-Efficient Fine-Tuning:** To efficiently adapt large-scale PLMs to downstream tasks, many adapter-tuning methods (Chen et al., 2023; He et al., 2023; Hu et al., 2021; Houlsby et al., 2019; Karimi Mahabadi et al., 2021; Liu et al., 2022) have been proposed. In general, adapter-tuning methods inject small, trainable, and task-specific adapter modules into each transformer layer of a pre-trained model. Given a pre-trained weight matrix  $W_0 \in \mathbb{R}^{d \times k}$  and input  $x \in \mathbb{R}^{k \times 1}$ , the weight update of adapter-tuning is expressed as  $W_0 + \Delta W$ . During training,  $W_0$  is frozen and does not receive gradient updates, while  $\Delta W$  contains trainable parameters. For  $h = W_0x$ , The modified forward pass in adapter-tuning yields:

$$h = W_0x + \Delta Wx. \quad (1)$$

To further improve parameter efficiency of adapter-tuning, AdaLoRA (Zhang et al., 2022) adaptively adjusts the number of trainable parameters among adapters according to their importance score — it reduces the number of trainable parameters for less important adapters. However, the adapter-tuning methods still use a large amount of memory, as shown in Figure 1, since they do not reduce the activation memory which accounts for a large portion of memory usage.

**Pruning LLM Model Parameters:** To reduce the model memory of fine-tuning, two categories of pruning methods have been proposed (Liang et al., 2021): structured pruning and unstructured pruning. Structured pruning methods remove grouped parameters (e.g., channels, layers) from the LLM.

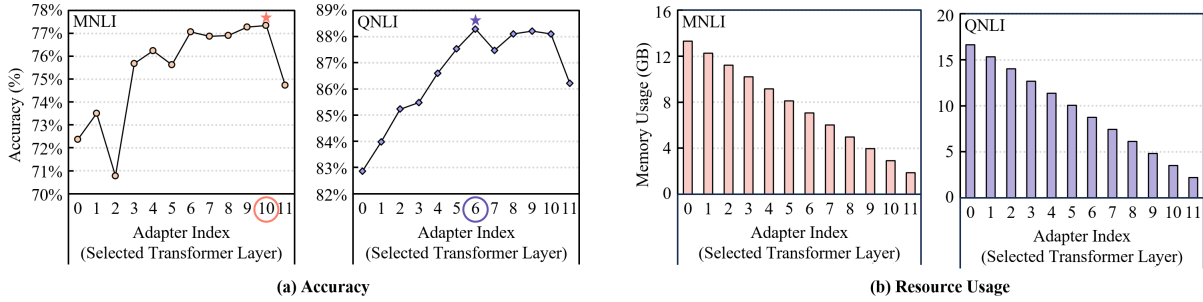


Figure 2: We quantify (a) accuracy and (b) memory usage of adapter-tuning by injecting an adapter into each transformer layer of BERT<sub>base</sub> model on MNL and QNLI dataset from GLUE.

However, they usually degrade the accuracy. Furthermore, they have a limitation in terms of the compression ratio because of the low flexibility. LLM-Pruner (Ma et al., 2023) compensates the accuracy drop coming from pruning, by employing post-training.

To overcome the limitation of structured pruning, unstructured pruning methods remove partial values of weight matrices regardless of their structures (Li et al., 2022b; Frantar and Alistarh, 2023). However, unstructured pruning also degrades the accuracy.

**Resource Efficient Fine-Tuning:** Several works have tried to target resource efficient fine-tuning. AdapterDrop (Rücklé et al., 2021), randomly excludes partial adapters from each training step. However, it cannot de-allocate the activation memory for the adapters, because of the random selections — an adapter excluded from training in a step can be included in training in the following steps. SparseAdapter (He et al., 2022) applies unstructured pruning to the adapters. However, it also does not reduce the actual memory usage — this is because the weight matrices pruned with zero values still need to be fully allocated in the memory. LoRAPrune (Zhang et al., 2023) employs structured pruning for LoRA. Unfortunately, the aforementioned methods usually have an adverse impact on the accuracy. MEFT (Liao et al., 2024) applies a reversible model to PEFT. By using the reversible network, MEFT calculates activations with accumulated outputs of layers, without saving the intermediate activations reducing the activation memory. However, calculations of the activations severely degrades the training time performance.

Different from the previous works, this work freezes less important adapters in early steps of training. Since the frozen adapters can only be used for the forward pass, early freezing of less

important adapters can effectively reduce the back-propagation length as well as the activation memory. Moreover, it induces regularization effect on the model, improving its accuracy.

### 3 Motivation

In this section, we present a pivotal research question for resource-efficient fine-tuning.

**RQ:** Do all adapters contribute equally to the process of adaptation?

To answer this question, we analyze the impact of adapters injected into each transformer layer on accuracy and resource efficiency. We measure the accuracy and memory usage of BERT<sub>base</sub> model on MNL and QNLI dataset from GLUE (Wang et al., 2018), by attaching an adapter to each transformer layer one-by-one. Figure 2(a) and (b) show the measured accuracy and memory usage respectively — the x-axis indicates the index of transformer layer that the adapter is injected into.

As shown in Figure 2(a), each adapter has different impact on the accuracy, and the importance of each adapter varies depending on the downstream task. In addition, despite uniform counts of trainable parameters, resource usage decreases for adapters closer to the output layer, as depicted in Figure 2(b). These observations point to the possibility that adapters in early layers contribute less to task adaptation, even though they require considerable resources. In other words, if we selectively deactivate less impactful adapters, it is possible to co-optimize the resource efficiency and accuracy.

To further analyze changes of the feature representations for each adapter throughout the training process, we quantify the representation similarity between adapters in each training step and those in the final model (which we obtained after the

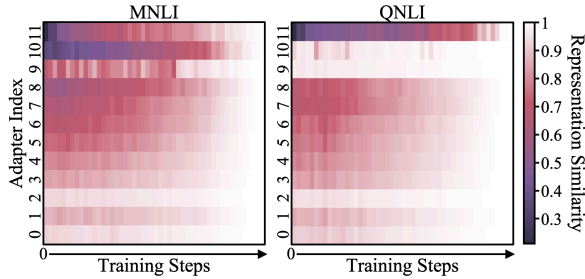


Figure 3: We visualize the representation similarity of the trained model and the model during training in adapter-tuning of the BERT<sub>base</sub> model on datasets from GLUE.

convergence of fine-tuning). We quantify the representational similarity using Centered Kernel Alignment (CKA) by referring to previous works (Li et al., 2022a). Figure 3 visualizes the representational similarity measured throughout the training process for each adapter for BERT<sub>base</sub> model on MNL and QNLI dataset from GLUE (Wang et al., 2018) — lighter the color becomes, higher the feature representation similarity is.

As shown in Figure 3, even in the early training steps, the feature representations of several adapters are almost the same as those of the final model — similar patterns are observed in other models and datasets. This means that those adapters are already representing the features that should be represented by the final model, and thus they may not further be adapted for the downstream task in the rest of the training steps. This is why such adapters are less contributing to the accuracy improvement of the model on the downstream tasks in Figure 2. One intuition is that lower adapters generally learn basic understanding of the input data, such as data bias and structural characteristics of the data, while adapters closer to the output build features unique to different tasks (Houlsby et al., 2019). Motivated by the observation where not all adapters consistently contribute to adaptation, in the next section, we propose a selective adapter freezing method which preemptively freezes adapters that are relatively less important for each task.

## 4 Selective Adapter Freezing (SAFE)

In this section, we propose a selective adapter freezing method, SAFE. SAFE adaptively freezes less important adapters in the early training steps, in order to reduce unnecessary computation and memory usage without compromising the accuracy.

Figure 4 shows the overview of SAFE. SAFE

consists of two stages: warm-up stage and freezing stage. In the warm-up stage, SAFE performs several epochs of fine-tuning while monitoring the feature representation changes (i.e., importance score) of the adapters (Section 4.1). If the importance score of all adapters is not much changed for consecutive epochs, SAFE enters the freezing stage. In the freezing stage, SAFE gradually freezes adapters that contribute less to the adaptation, based on the importance score (Section 4.2). By early freezing less important adapters, SAFE induces regularization effect on model (Section 4.3), leading to better performance.

### 4.1 Importance Score

In the warm-up stage<sup>1</sup>, we identify less important adapters by monitoring the feature representation changes of the adapters. To capture the feature representation changes of the adapters, SAFE uses Centered Kernel Alignment (CKA), which is a representative metric for representation similarity — similar practice has been used in previous works (Neysshabur et al., 2020; Raghu et al., 2021). It calculates CKA between the activation of a layer adapted with an adapter and that of the original layer as:

$$CKA_i(X_i, Y_i) = \frac{\|Y_i^T X_i\|_F^2}{\|X_i^T X_i\|_F \|Y_i^T Y_i\|_F}, \quad (2)$$

where  $X_i$  and  $Y_i$  are the activations of a layer that is adapted with an adapter and the original layer, respectively,  $i = \text{Index of Layer}$ , and  $\|\cdot\|_F^2$  represents the square of the Frobenius norm of a matrix.

Higher CKA value indicates that the feature representation of a layer is still similar with that of the original one. To this end, SAFE calculates the importance score of an adapter as:

$$Imp(Adapter_i) = 1 - CKA_i(X_i, Y_i) \quad (3)$$

### 4.2 Adapter Freezing

In the freezing stage, SAFE gradually freezes adapters based on their importance score. At  $t_w$ -th epoch, SAFE compares the importance score of adapters with threshold  $\tau_T$ . If the importance score of an adapter is lower than  $\tau_T$ , SAFE identifies the adapter as a freezing candidate. After identifying freezing candidates, SAFE gradually freezes them based on a moving threshold  $\tau_T$  until  $t_f$ -th epoch

<sup>1</sup>We define the number of warm-up epochs as the epoch at which the importance score of all adapters change by less than 5% for consecutive epochs.



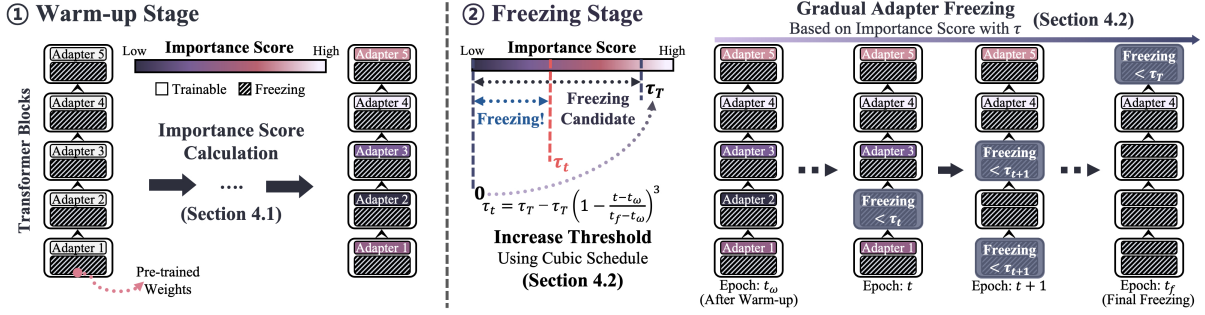


Figure 4: Design overview of Selective Adapter Freezing (SAFE). At the warm-up stage, SAFE identify important adapters by calculating importance score. At the freezing stage, SAFE gradually freezes the adapter based on their importance score with moving threshold  $\tau$  by following a cubic schedule.

— it increases 0 to  $\tau_T^2$  between  $t_w$ -th and  $t_f$ -th epochs following a cubic schedule as (Zhang et al., 2022):

$$\tau_t = \begin{cases} 0 & 0 \leq t < t_w, \\ \tau_T - \tau_T \left(1 - \frac{t - t_w}{t_f - t_w}\right)^3 & t_w \leq t < t_f, \\ \tau_T & \text{o.w.} \end{cases} \quad (4)$$

where  $t$  is the current epoch,  $t_w$  is the number of initial warm-up epochs,  $t_f$  is the number of final freezing epochs. This ensures that a large number of adapters participate in adaptation during the early stages of training, allowing SAFE to more accurately identify important adapters. As training progresses, less important adapters are gradually frozen, with different training periods assigned to each adapter based on their importance.

### 4.3 Regularization Effect of SAFE

By selectively freezing less critical adapters, SAFE induces a regularization effect within the model. In transformer-based PLM  $\mathcal{N}_0$ , each of the  $l$  transformer blocks  $T_l$  is equipped with a distinct set of parameters  $\theta_l^0$  for  $l \in \{1, \dots, n\}$ . To reduce the computational overhead of directly fine-tuning all parameters  $\theta_l^0$ , lightweight adapters  $\Delta\theta_l$  are introduced. To clarify how introducing adapters contributes to performance enhancements, Fu et al. (Fu et al., 2023) formalize the optimization function as follows:

$$\min_{\theta} \mathcal{L}(\theta) + \|(I - M)(\theta - \theta^0)\|^2, \quad (5)$$

where  $\theta = \theta^0 + M\Delta\theta$  and  $M \in \{0, 1\}^{m \times m}$ , with  $m = \dim(\theta)$ , serves as a diagonal matrix for selective parameter adjustment. Each diagonal element  $M_{ii} \in \{0, 1\}$  indicates whether the corresponding parameter of  $\Delta\theta_i$  is active (1) or inactive

<sup>2</sup>We empirically determine  $\tau_T$  and final freezing epochs  $t_f$  based on extensive experiments with various models and datasets.

(0), with all off-diagonal elements  $M_{ij}$  set to 0. The regularization term is crucial for explaining how parameter constraints introduced by adapters can enhance model performance on downstream tasks. The  $\text{rank}(M)$  is bounded by  $m$ , reflecting full capacity for parameter adaptation within each transformer block. However, such an approach can lead to excessive computation. In contrast, our study explores the implications of constraining the  $\text{rank}(M)$  to a reduced upper limit of  $\frac{m}{l}$  by selectively activating  $\Delta W_l$  for  $T_l$ . This constraint not only optimizes computational efficiency but also preserves the adaptability essential for superior performance on downstream tasks, as evidenced by our empirical results detailed in Section 5.3.

## 5 Experiments

### 5.1 Experimental Setting

**Models:** We assess the fine-tuning efficacy of SAFE using state-of-the-art transformer-based models, including BERT<sub>base</sub>, BERT<sub>large</sub> (Kenton and Toutanova, 2019), RoBERTa<sub>base</sub>, RoBERTa<sub>large</sub> (Liu et al., 2019), GPT-2<sub>medium</sub>, and GPT-2<sub>large</sub> (Radford et al., 2019).

**Datasets:** The aforementioned models are evaluated across various tasks that span a broad spectrum of NLP applications, including Natural Language Understanding (NLU), Question Answering (QA), and Natural Language Generation (NLG). Initially, we utilize eight datasets from the General Language Understanding Evaluation (GLUE) (Wang et al., 2018) which comprises two single-sentence classification tasks, three similarity and paraphrase tasks, and four natural language inference tasks. Furthermore, we conduct experiments on the SQuAD dataset (Rajpurkar et al., 2016) with both BERT and RoBERTa model families. Decoder-only models such as GPT-2<sub>large</sub> are also tested to

Table 1: Experimental results with BERT<sub>large</sub> on natural language understanding tasks from the GLUE benchmark. SAFE significantly reduces memory usage while achieving GLUE score comparable to the baseline. Note that we report memory usage and computation costs on RTE task.

	CoLA	SST-2	MNLI	RTE	QQP	MRPC	QNLI	STS-B	Avg.	Memory	Computation
	Matthews corr	Accuracy	Accuracy	Accuracy	Accuracy	F1 Score	Accuracy	Pearson corr		(GB)	(TFLOPs)
LoRA	65.24	93.65	85.40	72.66	90.49	87.90	90.06	91.88	84.66	20.35	46,698
+ AdapterDrop	64.24	92.54	85.19	73.38	89.02	86.51	91.51	91.39	84.22	20.35	35,114
+ SparseAdapter	65.25	92.66	85.19	74.10	90.43	88.50	91.61	91.99	84.97	20.35	46,698
+ SAFE	65.26	92.78	85.41	74.10	89.96	88.84	91.78	91.80	<b>84.99</b>	<b>12.11</b> 40.47%↓	<b>30,285</b> 35.15%↓

determine if SAFE maintains its effectiveness in the E2E NLG Challenge (Novikova et al., 2017). Detailed dataset descriptions are available in Appendix C.3.

**Baselines:** To evaluate the effectiveness of SAFE, we benchmark against state-of-the-art PEFT method, LoRA (Hu et al., 2021). We compare SAFE with two effective sparse training methods, AdapterDrop (Rücklé et al., 2021) and SparseAdapter (He et al., 2022). SAFE’s performance is further compared with other PEFT methods such as Houlsby (Houlsby et al., 2019), Pfeiffer (Pfeiffer et al., 2020), BitFit (Zaken et al., 2022), and the adaptive method AdaLoRA (Zhang et al., 2022) to demonstrate its versatility and applicability across different adapter-tuning frameworks (Figure 1, Appendix B). Comprehensive details on the experimental setup and hyperparameters, such as training epochs and batch sizes, can be found in Appendix C.

## 5.2 Main results

### 5.2.1 Natural Language Understanding

Table 1 shows the results of different methods on GLUE tasks. Since SAFE selectively freezes 51.04% of less important adapters early throughout the training process, SAFE significantly reduces memory usage by 40.47%, from 20.35GB (LoRA) to 12.11GB, and decreases computation costs (FLOPs) by 35.15%. Even with such improvements in resource efficiency, SAFE improves the average GLUE score from 84.66 (LoRA) to 84.99 — this is because SAFE induces a regularization effect on less-important adapters improving generalization performance of the model (see Section 5.3).

Compared to AdapterDrop, SAFE provides up to 2.69% higher score (MRPC) while reducing memory usage by 49.47% (0.91% higher GLUE score and 40.47% reduced memory usage on average).

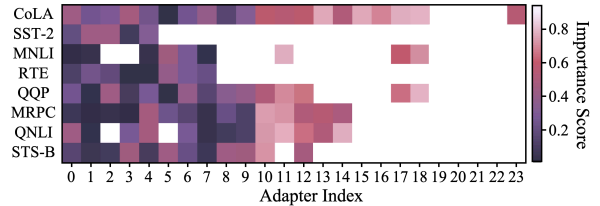


Figure 5: The freezing patterns when fine-tuning BERT<sub>large</sub> on GLUE with SAFE. Colors indicate adapters that are frozen, while white represents an adapter that is not frozen — the lighter the color is, the higher importance score is.

This is because AdapterDrop reduces computation costs (FLOPs) by randomly dropping adapters for each step, whereas SAFE selectively freezes less-important adapters preserving critical adapters and thus achieving better performance. AdapterDrop also does not lower memory usage because the memory allocated to the dropped adapters cannot be de-allocated for the next step — adapters dropped in a step may not be dropped in the next step. Compared to SparseAdapter, SAFE reduces memory usage by 40.47% and computation cost by 35.15% while providing comparable GLUE score. This is because SparseAdapter performs pruning of redundant parameters but uses unstructured pruning with masking, which does not actually improve resource efficiency.

Figure 5 shows the freezing patterns of BERT<sub>large</sub> fine-tuned with SAFE — we observe similar patterns for other tasks. We find that SAFE tends to freeze adapters more in layers closer to the input layer. Such behavior aligns with our empirical observations presented in Figure 2 where adapters closer to the output layer need to be further adapted to the downstream tasks compared to those in earlier layers, contributing more to model performance.

Table 2: Experimental results on question answering task from the SQuAD dataset.

		F1 Score	Memory Usage (GB)	Computation (TFLOPs)
BERT <sub>base</sub>	LoRA	86.99	5.95	611,295
	+ SAFE	<b>87.22</b>	<b>4.61</b> <sub>22.52% ↓</sub>	<b>455,274</b> <sub>25.52% ↓</sub>
BERT <sub>large</sub>	LoRA	89.22	15.79	2,117,791
	+ SAFE	<b>89.72</b>	<b>7.44</b> <sub>52.88% ↓</sub>	<b>869,624</b> <sub>58.94% ↓</sub>
RoBERTa <sub>base</sub>	LoRA	90.95	11.51	1,225,147
	+ SAFE	<b>91.16</b>	<b>7.80</b> <sub>32.23% ↓</sub>	<b>808,239</b> <sub>34.03% ↓</sub>
RoBERTa <sub>large</sub>	LoRA	93.39	17.73	2,117,791
	+ SAFE	<b>94.13</b>	<b>3.56</b> <sub>79.92% ↓</sub>	<b>245,541</b> <sub>88.41% ↓</sub>

### 5.2.2 Question Answering

Table 2 shows the results of SQuAD dataset. SAFE consistently outperforms baseline under all settings. Notably, SAFE reduces memory usage and computation costs by up to 79.92% and 88.41% on RoBERTa<sub>large</sub> by freezing 91.67% of the adapters, while improving the F1 score from 93.39 (LoRA) to 94.13. This result also demonstrates that the benefits and effectiveness of SAFE are not restricted to specific model sizes, making it a valuable strategy for enhancing adapter-tuning outcomes across models of varying scales.

### 5.2.3 Natural Language Generation

Table 3 shows that SAFE prevails on natural language generation task with GPT-2. SAFE achieves comparable performance to LoRA across all metrics while significantly reducing memory usage. This result also demonstrates that SAFE is effective not only for encoder models but also works well with decoder models.

To elucidate the underlying mechanisms behind SAFE’s enhancements in model performance and memory efficiency, we conduct a detailed empirical analysis. We visualize and compare the loss landscapes of the baseline and SAFE. Additionally, we quantitatively evaluate the flatness of the loss surfaces by analyzing the spectrum of Hessian eigenvalues. This methodical approach allows us to substantiate the improvements attributed to SAFE, providing insights into its effectiveness in optimizing both performance and resource utilization.

## 5.3 Regularization Effect

**Loss Landscape Analysis.** The flatness of a loss landscape is a recognized indicator of the generalization ability of models (Jiang et al., 2020). Specifically, flatter landscapes are indicative of enhanced robustness to parameter perturbations (Xie et al.,

Table 3: Experimental results on natural language generation from the E2E NLG Challenge. For all metrics, higher is better. We report memory usage reduction in blue.

		BLEU	NIST	METEOR	ROUGE-L	CIDEr
GPT-2 <sub>medium</sub>	LoRA	68.91	8.68	46.48	71.33	2.47
	+ SAFE	68.67	8.66	46.40	70.88	2.43
GPT-2 <sub>large</sub>	LoRA	70.27	8.85	46.40	71.63	2.52
	+ SAFE	70.26	8.87	46.58	71.68	2.53

2021), reduced model complexity (Blier and Olivier, 2018), and improved generalization capabilities (Cha et al., 2021, 2022; Choromanska et al., 2015; Park and Kim, 2021; Wu and Su, 2023). To examine these properties, we employ a comparative visualization of the loss landscapes for LoRA and SAFE using the BERT<sub>base</sub> model on the QNLI and SST-2 datasets, following the methodology outlined in (Park and Kim, 2021)<sup>3</sup>. Our analysis reveals that SAFE yields a flatter loss landscape compared to LoRA. This flattening is attributed to SAFE’s mechanism of controlling the norm of the weights through regularization effects (See Equation (5)), which consequently enhances resistance to weight perturbations, as depicted in Figure 6(a). **Hessian Eigenvalue Spectrum Analysis.** To quantitatively assess the visualized loss landscape shown in Figure 6(a), we perform a detailed analysis of the top-5 Hessian eigenvalue spectrum. A pivotal finding in our analysis is the reduced magnitude of the maximum Hessian eigenvalue, which correlates with a flatter loss landscape, indicative of enhanced generalization potential. Moreover, the diminution of large Hessian eigenvalues facilitates more effective model training (Ghorbani et al., 2019). Furthermore, the suppression of the largest *negative* Hessian eigenvalues markedly contributes to a more convex loss landscape, enhancing the stability of the training process. Figure 6(b) demonstrates that SAFE not only effectively reduces the magnitude of Hessian eigenvalues relative to LoRA but also leads to a smoother and more consistent loss landscape. This evidence highlights the advantages of SAFE in promoting a more reliable and steady training behavior for adapter-tuning.

<sup>3</sup>This involves generating two orthogonal random vectors in a 1D flattened parameter space, which are then normalized and used to perturb the parameters. The strength of these perturbations is determined by their  $x$  and  $y$  coordinates, with the origin (0, 0) representing the unperturbed state of the parameters, and increasing distance indicating greater perturbation intensity.

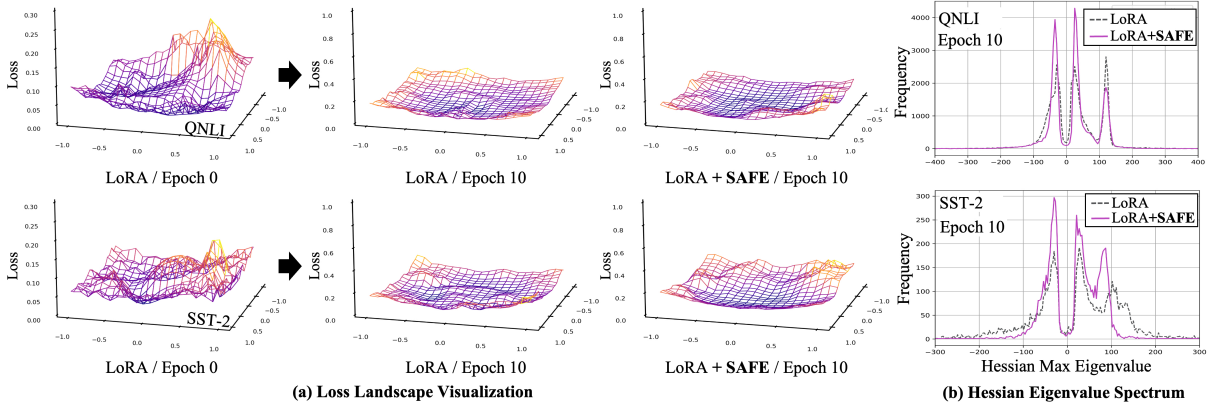


Figure 6: (a) Loss landscape demonstrates that SAFE yields a flatter loss surface compared to the baseline, as shown in the second and third columns. (b) Hessian eigenvalue spectrum analysis shows that the magnitude of the Hessian eigenvalues for SAFE is smaller than those for the baseline, indicating a flatter local curvature and potentially better generalization properties.

## 5.4 Resource Efficiency

We evaluate the resource efficiency of SAFE in terms of memory usage, computation amount, and training time. Table 4 shows the average resource efficiency improvement for the main results on NLU, QA and NLG tasks. Overall, SAFE reduces memory usage, computation amount, and training time by 42.85%, 34.59%, and 11.82% compared to LoRA, respectively (on average). This means that SAFE can fine-tune twice as many downstream tasks under the same FLOPs budget and further enable on-device fine-tuning for personalization. For example, when fine-tuning a  $\text{RoBERTa}_{\text{large}}$  model with a question answering downstream task, SAFE reduces memory usage from 17.73GB to 3.56GB; 8GB is the usual memory size of the edge devices.

## 5.5 Expanded Experimental Results

**Image Classification Task Evaluations.** In Appendix A, we conduct comprehensive evaluations of SAFE on a variety of image classification tasks. These experiments consistently demonstrate the efficacy of SAFE, confirming its robust performance across diverse vision-related applications.

**Compatibility with Advanced Adapters.** Further discussions on the integration of SAFE with various advanced adapter modules are presented in Appendix B. Our results highlight SAFE’s versatility and compatibility with multiple adapter-tuning frameworks (Houlsby et al., 2019; Zaken et al., 2022). This adaptability ensures that SAFE’s methodology remains effective, independent of specific adapter designs, thereby facilitating scalability

Table 4: SAFE improves efficiency over the baseline in all aspects including memory usage, computation amount and training time. Note that we report computation costs for 1-step training.

		NLU	QA	NLG
Memory Usage (GB)	LoRA	20.35	12.75	16.97
	+ SAFE	12.11 40.47%↓	5.85 54.08%↓	11.90 29.91%↓
Computational Cost (TFLOPs)	LoRA	1.24	5.94	8.64
	+ SAFE	0.93 24.74%↓	2.33 60.86%↓	6.79 21.42%↓
Training Time (Normalized)	LoRA	1	1	1
	+ SAFE	0.90 10.29%↓	0.89 10.92%↓	0.80 19.76%↓

across existing adapter-tuning methods.

## 6 Conclusion

In this paper, we propose SAFE, which selectively freezes adapters for enabling resource efficient fine-tuning of PLMs. We observe that not all adapters contribute equally to adaptation. Motivated by the observation, SAFE gradually freezes less-important adapters, which do not contribute to adaptation during the early training steps. In our evaluation on various models and datasets, SAFE significantly saves memory usage and computation and accelerating training time, with comparable (or even better) accuracy. We also demonstrate that SAFE induces regularization effect, thereby improving generalization performance and accuracy compared to the state-of-the-art PEFT methods. We believe that SAFE can enable resource-efficient fine-tuning of large-scale PLMs, and further pave the path forward to personalized fine-tuning on resource-constrained edge devices.



## 7 Limitations

We suggest the need for combination with prior research on memory-efficient training. These include low precision, microbatching, weight sharding, and gradient checkpointing techniques. Though we have not evaluated SAFE along with such memory-efficient training methods, SAFE can be complementarily used along with the methods since SAFE can be applied independently of the training method or weight precision. In particular, since the quantization-based compression technique is quite popular and effective in terms of both compression ratio and preservation of final accuracy, favorable results are expected from combining the proposed technique with the memory-efficient training methods (Han et al., 2015).

## References

- Léonard Blier and Yann Ollivier. 2018. The description length of deep learning models. *Advances in Neural Information Processing Systems*, 31.
- Lukas Bossard, Matthieu Guillaumin, and Luc Van Gool. 2014. Food-101—mining discriminative components with random forests. In *Computer Vision—ECCV 2014: 13th European Conference, Zurich, Switzerland, September 6–12, 2014, Proceedings, Part VI 13*, pages 446–461. Springer.
- Junbum Cha, Sanghyuk Chun, Kyungjae Lee, Hanchaeol Cho, Seunghyun Park, Yunsung Lee, and Sungrae Park. 2021. Swad: Domain generalization by seeking flat minima. *Advances in Neural Information Processing Systems*, 34:22405–22418.
- Junbum Cha, Kyungjae Lee, Sungrae Park, and Sanghyuk Chun. 2022. Domain generalization by mutual-information regularization with pre-trained models. In *European Conference on Computer Vision*, pages 440–457. Springer.
- Tianqi Chen, Bing Xu, Chiyuan Zhang, and Carlos Guestrin. 2016. Training deep nets with sublinear memory cost. *arXiv preprint arXiv:1604.06174*.
- Yukang Chen, Shengju Qian, Haotian Tang, Xin Lai, Zhijian Liu, Song Han, and Jiaya Jia. 2023. Longlora: Efficient fine-tuning of long-context large language models. In *The Twelfth International Conference on Learning Representations*.
- Anna Choromanska, Mikael Henaff, Michael Mathieu, Gérard Ben Arous, and Yann LeCun. 2015. The loss surfaces of multilayer networks. In *Artificial intelligence and statistics*, pages 192–204. PMLR.
- Elias Frantar and Dan Alistarh. 2023. Sparsegpt: Massive language models can be accurately pruned in one-shot. In *International Conference on Machine Learning*, pages 10323–10337. PMLR.

- Zihao Fu, Haoran Yang, Anthony Man-Cho So, Wai Lam, Lidong Bing, and Nigel Collier. 2023. On the effectiveness of parameter-efficient fine-tuning. In *Proceedings of the AAAI Conference on Artificial Intelligence*, volume 37, pages 12799–12807.
- Behrooz Ghorbani, Shankar Krishnan, and Ying Xiao. 2019. An investigation into neural net optimization via hessian eigenvalue density. In *International Conference on Machine Learning*, pages 2232–2241. PMLR.
- Song Han, Huizi Mao, and William J Dally. 2015. Deep compression: Compressing deep neural networks with pruning, trained quantization and Huffman coding. *arXiv preprint arXiv:1510.00149*.
- Shwai He, Liang Ding, Daize Dong, Jeremy Zhang, and Dacheng Tao. 2022. Sparseadapter: An easy approach for improving the parameter-efficiency of adapters. In *Findings of the Association for Computational Linguistics: EMNLP 2022*, pages 2184–2190.
- Xuehai He, Chunyuan Li, Pengchuan Zhang, Jianwei Yang, and Xin Eric Wang. 2023. Parameter-efficient model adaptation for vision transformers. In *Proceedings of the AAAI Conference on Artificial Intelligence*, volume 37, pages 817–825.
- Neil Houlsby, Andrei Giurgiu, Stanislaw Jastrzebski, Bruna Morrone, Quentin De Laroussilhe, Andrea Gesmundo, Mona Attariyan, and Sylvain Gelly. 2019. Parameter-efficient transfer learning for nlp. In *International Conference on Machine Learning*, pages 2790–2799. PMLR.
- Edward J Hu, Phillip Wallis, Zeyuan Allen-Zhu, Yuanzhi Li, Shean Wang, Lu Wang, Weizhu Chen, et al. 2021. Lora: Low-rank adaptation of large language models. In *International Conference on Learning Representations*.
- Yiding Jiang, Behnam Neyshabur, Hossein Mobahi, Dilip Krishnan, and Samy Bengio. 2020. Fantastic generalization measures and where to find them. In *International Conference on Learning Representations*.
- Rabeeh Karimi Mahabadi, James Henderson, and Sebastian Ruder. 2021. Compacter: Efficient low-rank hypercomplex adapter layers. *Advances in Neural Information Processing Systems*, 34:1022–1035.
- Jacob Devlin Ming-Wei Chang Kenton and Lee Kristina Toutanova. 2019. Bert: Pre-training of deep bidirectional transformers for language understanding. In *Proceedings of NAACL-HLT*, pages 4171–4186.
- Simon Kornblith, Mohammad Norouzi, Honglak Lee, and Geoffrey Hinton. 2019. Similarity of neural network representations revisited. In *International conference on machine learning*, pages 3519–3529. PMLR.

687	Jonathan Krause, Michael Stark, Jia Deng, and Li Fei-Fei. 2013. 3d object representations for fine-grained categorization. In <i>Proceedings of the IEEE international conference on computer vision workshops</i> , pages 554–561.	
688		
689		
690		
691		
692	Alex Krizhevsky et al. 2009. Learning multiple layers of features from tiny images.	
693		
694	Ya Le and Xuan Yang. Tiny imagenet visual recognition challenge.	
695		
696	Brian Lester, Rami Al-Rfou, and Noah Constant. 2021. The power of scale for parameter-efficient prompt tuning. In <i>Proceedings of the 2021 Conference on Empirical Methods in Natural Language Processing</i> , pages 3045–3059.	
697		
698		
699		
700		
701	Sheng Li, Geng Yuan, Yue Dai, Youtao Zhang, Yanzhi Wang, and Xulong Tang. 2022a. Smartfrz: An efficient training framework using attention-based layer freezing. In <i>The Eleventh International Conference on Learning Representations</i> .	
702		
703		
704		
705		
706	Xiang Lisa Li and Percy Liang. 2021. Prefix-tuning: Optimizing continuous prompts for generation. In <i>Proceedings of the 59th Annual Meeting of the Association for Computational Linguistics and the 11th International Joint Conference on Natural Language Processing (Volume 1: Long Papers)</i> , pages 4582–4597.	
707		
708		
709		
710		
711		
712		
713	Yuchao Li, Fuli Luo, Chuanqi Tan, Mengdi Wang, Songfang Huang, Shen Li, and Junjie Bai. 2022b. Parameter-efficient sparsity for large language models fine-tuning. <i>arXiv preprint arXiv:2205.11005</i> .	
714		
715		
716		
717	Tailin Liang, John Glossner, Lei Wang, Shaobo Shi, and Xiaotong Zhang. 2021. Pruning and quantization for deep neural network acceleration: A survey. <i>Neurocomputing</i> , 461:370–403.	
718		
719		
720		
721	Baohao Liao, Shaomu Tan, and Christof Monz. 2024. Make pre-trained model reversible: From parameter to memory efficient fine-tuning. <i>Advances in Neural Information Processing Systems</i> , 36.	
722		
723		
724		
725	Haokun Liu, Derek Tam, Mohammed Muqeeth, Jay Mohata, Tenghao Huang, Mohit Bansal, and Colin Raffel. 2022. Few-shot parameter-efficient fine-tuning is better and cheaper than in-context learning. <i>Advances in Neural Information Processing Systems</i> , 35:1950–1965.	
726		
727		
728		
729		
730		
731	Xiao Liu, Yanan Zheng, Zhengxiao Du, Ming Ding, Yujie Qian, Zhilin Yang, and Jie Tang. 2023. Gpt understands, too. <i>AI Open</i> .	
732		
733		
734	Yinhan Liu, Myle Ott, Naman Goyal, Jingfei Du, Mandar Joshi, Danqi Chen, Omer Levy, Mike Lewis, Luke Zettlemoyer, and Veselin Stoyanov. 2019. Roberta: A robustly optimized bert pretraining approach. <i>arXiv preprint arXiv:1907.11692</i> .	
735		
736		
737		
738		
739	Ilya Loshchilov and Frank Hutter. 2018. Decoupled weight decay regularization. In <i>International Conference on Learning Representations</i> .	
740		
741		
	Xinyin Ma, Gongfan Fang, and Xinchao Wang. 2023. Llm-pruner: On the structural pruning of large language models. <i>Advances in neural information processing systems</i> , 36:21702–21720.	742
		743
		744
		745
	Behnam Neyshabur, Hanie Sedghi, and Chiyuan Zhang. 2020. What is being transferred in transfer learning? <i>Advances in neural information processing systems</i> , 33:512–523.	746
		747
		748
		749
	Maria-Elena Nilsback and Andrew Zisserman. 2008. Automated flower classification over a large number of classes. In <i>2008 Sixth Indian conference on computer vision, graphics &amp; image processing</i> , pages 722–729. IEEE.	750
		751
		752
		753
		754
	Jekaterina Novikova, Ondrej Dusek, and Verena Rieser. 2017. The e2e dataset: New challenges for end-to-end generation. In <i>18th Annual Meeting of the Special Interest Group on Discourse and Dialogue</i> , pages 201–206. Association for Computational Linguistics.	755
		756
		757
		758
		759
		760
	Namuk Park and Songkuk Kim. 2021. How do vision transformers work? In <i>International Conference on Learning Representations</i> .	761
		762
		763
	Jonas Pfeiffer, Aishwarya Kamath, Andreas Rücklé, Kyunghyun Cho, and Iryna Gurevych. 2021. Adapterfusion: Non-destructive task composition for transfer learning. In <i>Proceedings of the 16th Conference of the European Chapter of the Association for Computational Linguistics: Main Volume</i> , pages 487–503.	764
		765
		766
		767
		768
		769
		770
	Jonas Pfeiffer, Andreas Rücklé, Clifton Poth, Aishwarya Kamath, Ivan Vulić, Sebastian Ruder, Kyunghyun Cho, and Iryna Gurevych. 2020. Adapterhub: A framework for adapting transformers. In <i>Proceedings of the 2020 Conference on Empirical Methods in Natural Language Processing: System Demonstrations</i> , pages 46–54.	771
		772
		773
		774
		775
		776
		777
	Alec Radford, Jong Wook Kim, Chris Hallacy, Aditya Ramesh, Gabriel Goh, Sandhini Agarwal, Girish Sastry, Amanda Askell, Pamela Mishkin, Jack Clark, et al. 2021. Learning transferable visual models from natural language supervision. In <i>International conference on machine learning</i> , pages 8748–8763. PMLR.	778
		779
		780
		781
		782
		783
	Alec Radford, Jeffrey Wu, Rewon Child, David Luan, Dario Amodei, Ilya Sutskever, et al. 2019. Language models are unsupervised multitask learners. <i>OpenAI blog</i> , 1(8):9.	784
		785
		786
		787
	Maithra Raghu, Thomas Unterthiner, Simon Kornblith, Chiyuan Zhang, and Alexey Dosovitskiy. 2021. Do vision transformers see like convolutional neural networks? <i>Advances in neural information processing systems</i> , 34:12116–12128.	788
		789
		790
		791
		792
	Pranav Rajpurkar, Jian Zhang, Konstantin Lopyrev, and Percy Liang. 2016. Squad: 100,000+ questions for machine comprehension of text. In <i>Proceedings of the 2016 Conference on Empirical Methods in Natural Language Processing</i> , pages 2383–2392.	793
		794
		795
		796
		797

798	Minsoo Rhu, Natalia Gimelshein, Jason Clemons,	2023. Loraprune: Pruning meets low-rank parameter-	854
799	Arslan Zulfiqar, and Stephen W Keckler. 2016.	efficient fine-tuning.	855
800	vdnn: Virtualized deep neural networks for scalable,		
801	memory-efficient neural network design. In <i>2016</i>	Qingru Zhang, Minshuo Chen, Alexander Bukharin,	856
802	<i>49th Annual IEEE/ACM International Symposium on</i>	Pengcheng He, Yu Cheng, Weizhu Chen, and	857
803	<i>Microarchitecture (MICRO)</i> , pages 1–13. IEEE.	Tuo Zhao. 2022. Adaptive budget allocation for	858
		parameter-efficient fine-tuning. In <i>The Eleventh In-</i>	859
804	Andreas Rücklé, Gregor Geigle, Max Glockner, Tilman	<i>ternational Conference on Learning Representations.</i>	860
805	Beck, Jonas Pfeiffer, Nils Reimers, and Iryna		
806	Gurevych. 2021. Adapterdrop: On the efficiency		
807	of adapters in transformers. In <i>Proceedings of the</i>		
808	<i>2021 Conference on Empirical Methods in Natural</i>		
809	<i>Language Processing</i> , pages 7930–7946.		
810	Hugo Touvron, Thibaut Lavril, Gautier Izacard, Xavier		
811	Martinet, Marie-Anne Lachaux, Timothée Lacroix,		
812	Baptiste Rozière, Naman Goyal, Eric Hambro,		
813	Faisal Azhar, et al. 2023. Llama: Open and effi-		
814	cient foundation language models. <i>arXiv preprint</i>		
815	<i>arXiv:2302.13971</i> .		
816	Alex Wang, Amanpreet Singh, Julian Michael, Felix		
817	Hill, Omer Levy, and Samuel Bowman. 2018. Glue:		
818	A multi-task benchmark and analysis platform for		
819	natural language understanding. In <i>Proceedings of</i>		
820	<i>the 2018 EMNLP Workshop BlackboxNLP: Analyz-</i>		
821	<i>ing and Interpreting Neural Networks for NLP</i> , pages		
822	353–355.		
823	Thomas Wolf, Lysandre Debut, Victor Sanh, Julien		
824	Chaumond, Clement Delangue, Anthony Moi, Pier-		
825	ric Cistac, Tim Rault, Rémi Louf, Morgan Funtowicz,		
826	et al. 2019. Huggingface’s transformers: State-of-		
827	the-art natural language processing. <i>arXiv preprint</i>		
828	<i>arXiv:1910.03771</i> .		
829	Lei Wu and Weijie J Su. 2023. The implicit regular-		
830	ization of dynamical stability in stochastic gradient		
831	descent. <i>arXiv preprint arXiv:2305.17490</i> .		
832	Han Xiao, Kashif Rasul, and Roland Vollgraf. 2017.		
833	Fashion-mnist: a novel image dataset for benchmark-		
834	ing machine learning algorithms. <i>arXiv preprint</i>		
835	<i>arXiv:1708.07747</i> .		
836	Zeke Xie, Fengxiang He, Shaopeng Fu, Issei Sato,		
837	Dacheng Tao, and Masashi Sugiyama. 2021. Arti-		
838	ficial neural variability for deep learning: On overfit-		
839	ting, noise memorization, and catastrophic forgetting.		
840	<i>Neural computation</i> , 33(8):2163–2192.		
841	Zhilin Yang, Zihang Dai, Yiming Yang, Jaime Car-		
842	bonell, Russ R Salakhutdinov, and Quoc V Le. 2019.		
843	Xlnet: Generalized autoregressive pretraining for lan-		
844	guage understanding. <i>Advances in neural informa-</i>		
845	<i>tion processing systems</i> , 32.		
846	Elad Ben Zaken, Yoav Goldberg, and Shauli Ravfogel.		
847	2022. Bitfit: Simple parameter-efficient fine-tuning		
848	for transformer-based masked language-models. In		
849	<i>Proceedings of the 60th Annual Meeting of the As-</i>		
850	<i>sociation for Computational Linguistics (Volume 2:</i>		
851	<i>Short Papers)</i> , pages 1–9.		
852	Mingyang Zhang, Hao Chen, Chunhua Shen, Zhen		
853	Yang, Linlin Ou, Xinyi Yu, and Bohan Zhuang.		

## A Results on Image Classification Tasks

We conduct experiments with 8 datasets including class-level transfer and task-level transfer in the image classification tasks within Computer Vision (CV) domain. These datasets include CIFAR-10, CIFAR-100 (Krizhevsky et al., 2009), Country-211 (Radford et al., 2021), Fashion MNIST (Xiao et al., 2017), Food-101 (Bossard et al., 2014), Oxford Flowers (Nilsback and Zisserman, 2008), Stanford Cars (Krause et al., 2013) and Tiny ImageNet (Le and Yang).

Table 5 shows that SAFE can effectively reduce memory usage while achieving comparable accuracy on eight datasets in the image classification task. For example, SAFE achieves a 50.69% memory usage reduction on ViT<sub>large</sub> while maintaining comparable accuracy. Additionally, SAFE remains consistently effective regardless of variations in the pre-trained model size and backbone structure.

Table 5: Experimental results on eight common computer vision tasks. SAFE significantly reduces memory usage while achieving accuracy comparable to the baseline. Note that blue indicates the memory usage reduction rate of SAFE compared to the baseline.

		CIFAR-10	CIFAR-100	Country-211	Fashion MNIST	Food-101	Oxford Flowers	Stanford Cars	Tiny ImageNet	Avg.
ViT <sub>base</sub>	LoRA	97.77	95.68	16.56	94.52	88.84	99.41	82.56	88.90	<b>83.03</b>
	+ SAFE	98.66	95.55	16.29	93.71	88.78	99.61	82.05	89.16	82.98 <b>24.35%↓</b>
ViT <sub>large</sub>	LoRA	99.09	96.71	20.44	94.92	90.32	-	86.97	92.13	82.94
	+ LoRA	99.13	97.00	20.44	94.88	90.69	-	86.83	92.03	<b>83.00</b> <b>50.69%↓</b>
SWIN <sub>base</sub>	LoRA	98.92	96.20	20.06	95.12	91.36	99.50	87.14	90.31	84.83
	+ SAFE	98.94	96.31	20.26	95.12	91.51	99.71	86.88	90.14	<b>84.86</b> <b>32.01%↓</b>
SWIN <sub>large</sub>	LoRA	99.07	97.01	22.19	95.44	92.68	-	85.06	92.02	83.35
	+ LoRA	99.17	96.72	22.66	95.47	92.69	-	85.13	92.11	<b>83.42</b> <b>25.06%↓</b>

## B Results with Various PEFT Methods

We validate the applicability of SAFE upon advanced adapter modules (Houlsby et al., 2019; Zaken et al., 2022; Hu et al., 2021). Table 6 shows that SAFE reduces memory usage by 24.76% on average while achieving a comparable GLUE score. This result demonstrates that SAFE can be applied to a variety of adapter-tuning methods to enable resource efficient fine-tuning of large language models.

Table 6: Experimental results for various adapter-tuning methods on the GLUE benchmark. Note that blue indicates the memory usage reduction rate of SAFE compared to the baseline.

	CoLA	SST-2	MNLI	RTE	QQP	MRPC	QNLI	STS-B	Avg.
BERT <sub>base</sub>	Matthews corr.	Accuracy	Accuracy	Accuracy	Accuracy	F1 Score	Accuracy	Pearson corr.	
Houlsby	62.38	91.17	83.44	70.50	90.85	89.52	90.59	90.75	83.65
+ SAFE	62.83	93.00	84.15	74.10	90.93	89.70	91.03	91.29	<b>84.63</b> <b>25.70%↓</b>
BitFit	60.92	91.86	82.41	71.94	89.20	88.14	89.80	90.95	<b>83.15</b>
+ SAFE	61.73	93.00	81.85	69.78	89.21	88.85	89.51	90.75	83.09 <b>25.53%↓</b>
LoRA	64.46	91.63	82.88	71.22	90.01	88.39	90.01	90.86	83.68
+ SAFE	66.80	90.83	82.03	71.22	89.74	88.51	90.65	90.26	<b>83.76</b> <b>23.06%↓</b>



## C Experimental Setup

### C.1 Model

We conduct experiments using a pre-trained model deployed on HuggingFace (Wolf et al., 2019). For experiments on the NLU and QA benchmarks, we use bert-base-uncased and bert-large-uncased trained on BookCorpus, a dataset consisting of 11,038 unpublished books and English Wikipedia. We use roberta-base and roberta-large trained on 5 datasets (BookCorpus, English Wikipedia, CC-News, OpenWebText, and Stories) for the RoBERTa model. For experiments on the NLG benchmark, we use GPT-2 medium and GPT-2 large distributed by OpenAI. We use vit-base-patch16-224-in21k and vit-large-patch16-224-in21k distributed by Google for experiments in the ViT model. Finally, We use the swin-base-patch4-window7-224 and swin-large-patch4-window7-224 models distributed by Microsoft for experiments in the SWIN model.

### C.2 Computing Resources

Our experimental setup leverages 2 RTX4090 with 24GB memory for NLU, QA, and NLG tasks and 1 RTX 4090 for CV downstream task.

### C.3 Dataset Statistics

We present the dataset statistics of GLUE and SQuAD in following table.

Table 7: Summary of the NLP and QA benchmarks.

NLU Benchmark						
Dataset	# Train	# Valid	# Test	# Label	Task	Evaluation Metric
Single-Sentence Classification (GLUE)						
CoLA	8,551	521	522	2	Acceptability	Matthews corr
SST-2	66,349	1,000	872	2	Sentiment	Accuracy
Pairwise Text Classification (GLUE)						
MNLI	392,702	9,832	9,815	3	NLI	Accuracy
RTE	2,490	138	139	2	NLI	Accuracy
QQP	362,846	1,000	40,431	2	Paraphrase	Accuracy
MRPC	3,668	204	204	2	Paraphrase	F1 score
QNLI	103,743	1,000	5,463	2	QA/NLI	Accuracy
Pairwise Text Classification (GLUE)						
STS-B	5,749	750	750	1	Similarity	Pearson corr
QA Benchmark						
Dataset	# Train	# Valid	# Test	# Label	Task	Evaluation Metric
SQuAD	87,600	5,300	5,300	2	Question Answering	F1 score
NLG Benchmark						
Dataset	# Train	# Valid	# Test	# Label	Task	Evaluation Metric
E2E NLG Challenge	42,061	4,672	4,693		Generation	BLEU, NIST, METEOR, ROUGE-L, and CIDEr

The following table lists dataset statistics evaluated in the CV domain.

Table 8: Summary of CV benchmark.

CV Benchmark						
Dataset	# Train	# Valid	# Test	# Label	Task	Evaluation Metric
CIFAR-10	45,000	5,000	10,000	10	Classification	Accuracy
CIFAR-100	45,000	5,000	10,000	100	Classification	Accuracy
Fashion MNIST	54,000	6,000	10,000	10	Classification	Accuracy
Oxford Flowers	6,453	717	1,020	102	Classification	Accuracy
Food-101	68,220	7,580	25,300	102	Classification	Accuracy
Country-211	25,920	2,880	21,100	211	Classification	Accuracy
Stanford Cars	7,326	814	8,040	196	Classification	Accuracy
Tiny ImageNet	90,000	10,000	10,000	200	Classification	Accuracy

893  
894  
895  
896  
897  
898

### C.4 Hyperparameter Settings

We explore 10% of all epochs for at least 5 learning rates. Hyperparameter settings, including learning rate, are made by referring to previous works (He et al., 2023; Houlsby et al., 2019; Hu et al., 2021; Zaken et al., 2022). We use the AdamW optimizer (Loshchilov and Hutter, 2018) and LinearLR learning rate scheduler and set weight decay to 0 in experiments. In our evaluation, we configure LoRA as follows:  $r = 4$ ,  $\alpha = 16$ , target modules = ["query", "value"], and LoRA dropout = 0.1.

Table 9: Hyperparameter settings on the NLU and QA tasks.

pre-trained model	dataset	method	final learning rate	batch size	# epochs
<b>BERT-base-uncased</b>	GLUE / CoLA	LoRA, LoRA + SAFE	6.00E-04	32	100
		BitFit, BitFit + SAFE	9.00E-04	32	100
		Houlsby, Houlsby + SAFE	5.00E-04	32	100
	GLUE / SST-2	LoRA, LoRA + SAFE	7.00E-04	32	75
		BitFit, BitFit + SAFE	7.00E-04	32	75
		Houlsby, Houlsby + SAFE	2.00E-04	32	75
	GLUE / MNLI	LoRA, LoRA + SAFE	9.00E-04	32	50
		BitFit, BitFit + SAFE	8.00E-04	32	50
		Houlsby, Houlsby + SAFE	4.00E-04	32	50
	GLUE / RTE	LoRA, LoRA + SAFE	9.00E-04	32	100
		BitFit, BitFit + SAFE	8.00E-04	32	100
		Houlsby, Houlsby + SAFE	4.00E-04	32	100
	GLUE / QQP	LoRA, LoRA + SAFE	4.00E-04	32	50
		BitFit, BitFit + SAFE	6.00E-04	32	50
		Houlsby, Houlsby + SAFE	4.00E-04	32	50
	GLUE / MRPC	LoRA, LoRA + SAFE	5.00E-04	16	50
		BitFit, BitFit + SAFE	5.00E-04	32	50
		Houlsby, Houlsby + SAFE	5.00E-04	32	50
	GLUE / QNLI	LoRA, LoRA + SAFE	5.00E-04	32	50
		BitFit, BitFit + SAFE	5.00E-04	32	50
		Houlsby, Houlsby + SAFE	4.00E-04	32	50
	GLUE / STS-B	LoRA, LoRA + SAFE	8.00E-04	32	50
		BitFit, BitFit + SAFE	9.00E-04	32	50
		Houlsby, Houlsby + SAFE	5.00E-04	32	50
SQuAD	LoRA, LoRA + SAFE	3.00E-04	16	50	
	BitFit, BitFit + SAFE	9.00E-04	16	50	
	Houlsby, Houlsby + SAFE	1.00E-04	16	50	
<b>BERT-large-uncased</b>	GLUE / CoLA	LoRA, LoRA + SAFE	1.00E-04	32	80
	GLUE / SST-2	LoRA, LoRA + SAFE	6.00E-04	32	60
	GLUE / MNLI	LoRA, LoRA + SAFE	1.00E-04	16	40
	GLUE / RTE	LoRA, LoRA + SAFE	6.00E-04	32	80
	GLUE / QQP	LoRA, LoRA + SAFE	3.00E-04	16	40
	GLUE / MRPC	LoRA, LoRA + SAFE	3.00E-04	4	50
	GLUE / QNLI	LoRA, LoRA + SAFE	2.00E-04	8	50
	GLUE / STS-B	LoRA, LoRA + SAFE	8.00E-04	32	50
		Full-param Fine-tuning	7.00E-05	16	50
		LoRA, LoRA + SAFE	3.00E-04	16	50
	SQuAD	BitFit, BitFit + SAFE	9.00E-04	16	50
		Houlsby, Houlsby + SAFE	1.00E-04	16	50
		Pfeiffer, Pfeiffer + SAFE	3.00E-04	16	50
		AdaLoRA, AdaLoRA + SAFE	4.00E-04	16	50
	<b>RoBERTa-base</b>	SQuAD	LoRA, LoRA + SAFE	5.00E-04	32
BitFit, BitFit+SAFE			8.00E-04	32	50
Houlsby, Houlsby+SAFE			4.00E-04	32	50
<b>RoBERTa-large</b>	SQuAD	LoRA, LoRA + SAFE	6.00E-04	16	50
		BitFit, BitFit+SAFE	7.00E-04	16	50
		Houlsby, Houlsby+SAFE	4.00E-04	16	50

Table 10: Hyperparameter settings on the NLG task.

pre-trained model	GPT-2 medium	GPT-2 large
Training		
final learning rate	1.00E-04	5.00E-05
batch size	8	4
# epochs	10	10
Seq Length	512	512
Label Smooth	0.1	0.1
Inference		
Beam Size	10	10
Length Penalty	0.8	0.8
no repeat ngram size	4	4

Table 11: Hyperparameter settings on the CV task.

pre-trained model	dataset	method	final learning rate	batch size	# epochs
<b>ViT-base-patch16-224</b>	CIFAR-10	BitFit, BitFit + SAFE	3.00E-03	64	100
		LoRA, LoRA + SAFE	3.00E-03	64	100
	CIFAR-100	BitFit, BitFit + SAFE	3.00E-03	64	100
		LoRA, LoRA + SAFE	3.00E-03	64	100
	Fashion MNIST	BitFit, BitFit + SAFE	4.00E-03	64	100
		LoRA, LoRA + SAFE	3.00E-03	64	100
	Oxford Flowers	BitFit, BitFit + SAFE	2.00E-03	64	30
		LoRA, LoRA + SAFE	8.00E-04	64	40
	Food-101	BitFit, BitFit + SAFE	4.00E-03	64	100
		LoRA, LoRA + SAFE	3.00E-03	64	100
	Tiny ImageNet	BitFit, BitFit + SAFE	1.00E-03	64	100
		LoRA, LoRA + SAFE	8.00E-04	64	100
	Country-211	BitFit, BitFit + SAFE	2.00E-03	64	100
		LoRA, LoRA + SAFE	4.00E-03	64	100
	Stanford Cars	BitFit, BitFit + SAFE	9.00E-03	64	100
		LoRA, LoRA + SAFE	7.00E-03	64	100
<b>ViT-large-patch16-224</b>	CIFAR-10	BitFit, BitFit + SAFE	4.00E-03	64	100
		LoRA, LoRA + SAFE	6.00E-04	64	100
	CIFAR-100	BitFit, BitFit + SAFE	2.00E-03	64	100
		LoRA, LoRA + SAFE	5.00E-04	64	100
	Fashion MNIST	BitFit, BitFit + SAFE	3.00E-03	64	100
		LoRA, LoRA + SAFE	9.00E-04	64	100
	Oxford Flowers	BitFit, BitFit + SAFE	-	-	-
		LoRA, LoRA + SAFE	-	-	-
	Food-101	BitFit, BitFit + SAFE	9.00E-04	64	100
		LoRA, LoRA + SAFE	7.00E-04	64	100
	Tiny ImageNet	BitFit, BitFit + SAFE	8.00E-04	64	100
		LoRA, LoRA + SAFE	6.00E-04	64	100
	Country-211	BitFit, BitFit + SAFE	2.00E-03	64	100
		LoRA, LoRA + SAFE	9.00E-04	64	100
	Stanford Cars	BitFit, BitFit + SAFE	1.00E-03	64	100
		LoRA, LoRA + SAFE	1.00E-03	64	100
<b>SWIN-base-patch4-window7-224</b>	CIFAR-10	LoRA, LoRA + SAFE	1.00E-03	64	50
	CIFAR-100	LoRA, LoRA + SAFE	1.00E-03	64	50
	Fashion MNIST	LoRA, LoRA + SAFE	1.00E-03	64	50
	Oxford Flowers	LoRA, LoRA + SAFE	7.00E-04	64	30
	Food-101	LoRA, LoRA + SAFE	9.00E-04	64	50
	Tiny ImageNet	LoRA, LoRA + SAFE	1.00E-03	64	50
	Country-211	LoRA, LoRA + SAFE	7.00E-04	64	50
	Stanford Cars	LoRA, LoRA + SAFE	1.00E-03	64	50
<b>SWIN-large-patch4-window7-224</b>	CIFAR-10	LoRA, LoRA + SAFE	8.00E-04	64	50
	CIFAR-100	LoRA, LoRA + SAFE	7.00E-04	64	50
	Fashion MNIST	LoRA, LoRA + SAFE	1.00E-03	64	50
	Oxford Flowers	LoRA, LoRA + SAFE	-	-	-
	Food-101	LoRA, LoRA + SAFE	5.00E-04	64	50
	Tiny ImageNet	LoRA, LoRA + SAFE	6.00E-04	64	50
	Country-211	LoRA, LoRA + SAFE	6.00E-04	64	50
	Stanford Cars	LoRA, LoRA + SAFE	3.00E-03	64	50